Surrogate Modelling for the Seismic Performance Assessment of Liquid Storage Tanks[1]

Konstantinos Bakalis[2], Michalis Fragiadakis[3] and Dimitrios Vamvatsikos[4]

Abstract: A three-dimensional surrogate model is presented for the seismic performance assessment of cylindrical atmospheric liquid storage tanks. The proposed model consists of a concentrated fluid mass attached to a single vertical beam-column element, that rests on rigid beam-spokes with edge springs. The model is suitable for rapid static and dynamic seismic performance assessment. Contrary to other simplified models for tanks, its properties are determined through simple structural analysis that can be performed in any nonlinear analysis software, without the need for complex finite element models. The results compare favorably to those of three-dimensional finite element models on three tanks of varying aspect ratios. A step-by-step example of the modelling procedure is presented for a squat unanchored tank, and a sensitivity analysis is conducted in order to investigate the effect of various modelling parameters on the seismic response of the proposed tank model.

CE Database subject headings: Seismic response; Earthquakes; Performance evaluation;

Author Keywords: Performance-based Earthquake Engineering; Liquid Storage Tanks; Nonlinear Analysis;

Introduction

Large-capacity atmospheric tanks are typical structures of the chemical industry that are widely used to store a variety of liquids, such as oil or liquefied natural gas. The seismic risk of such industrial facilities is considerably higher compared to ordinary structures, since even some minor damage induced by a ground motion may have uncontrollable consequences, not only on the tank but also on the environment. Recent earthquakes have shown that heavy damage on tanks may lead to temporary loss of essential service, usually followed by leakage and/or fire (Girgin 2011; Hatayama 2015). Despite extensive research, earthquakes remain a major threat for the structures both from a social and a financial point of view.

The Performance-Based Earthquake Engineering (PBEE) concept can be employed to better understand and quantify the seismic performance of such critical infrastructure. Appropriate structural models are essential for the successful seismic performance

---

[1] Based on two short papers presented at the 2nd European Conference on Earthquake Engineering and Seismology, Istanbul, Turkey, 2014 and the 8th Hellenic National Conference of Steel Structures Tripoli, Greece, 2014.

[2] PhD Student, School of Civil Engineering, National Technical Univ. of Athens, Greece (corresponding author). E-mail: kbakalis@mail.ntua.gr

[3] Assistant Professor, School of Civil Engineering, National Technical Univ. of Athens, Greece. E-mail: mfrag@mail.ntua.gr

[4] Assistant Professor, School of Civil Engineering, National Technical Univ. of Athens, Greece. E-mail: divamva@mail.ntua.gr

evaluation. Especially for atmospheric liquid storage tanks, detailed finite element models (FEM) require a considerable amount of time even for a single dynamic analysis (Kilic and Ozdemir 2007), while capturing the fluid-structure-interaction effect is an onerous task. Although FEM-based procedures may be able to capture complex modes of failure such as buckling (Buratti and Tavano 2014; Virella et al. 2006), their suitability within a probabilistic seismic performance assessment framework may become computationally prohibitive.

Other studies regarding the response of liquid storage tanks have either developed or adopted numerical approximations for the contained liquid (Ahari et al. 2009; Talaslidis et al. 2004; Vathi et al. 2013) in an attempt to minimize the computational time. Simplified modelling techniques that blend efficiency and accuracy are offered by Malhotra and Veletsos (1994a; b; c), who presented a simplified model for the analysis of liquid storage tanks subject to a single component of ground motion (essentially two-dimensional (2D) formulation). Furthermore, Cortes et al. (2012) also developed a 2D model based on rigid beams and equivalent springs that can be used for rapid response history analysis. The aforementioned approaches cannot be applied with typical commercial structural analysis software. The first approach requires a dedicated analysis algorithm that is not generally available, while the second needs to be calibrated using FEM results.

Building upon the approach of Malhotra and Veletsos, a more sophisticated model that relies on beam-column elements and point springs available in most structural analysis packages, is offered instead. The aim is to develop a three-dimensional (3D) surrogate model that can be subjected to all translational components of ground motion and can be implemented with minimum effort both for anchored and unanchored tanks, using either static or dynamic analysis. The efficiency of the model is assessed with the aid of detailed FE results, while a sensitivity analysis is performed in order to understand the influence of the various properties of the proposed model on its response estimates.

Modelling of Liquid Storage Tanks

Background

Modelling of liquid storage tanks is a challenging problem as it requires capturing the dynamic response of the contained fluid and its interaction with the tank walls. The hydrodynamic problem can be summarized in the combination of an impulsive and a convective component (Veletsos and Tang 1990). Part of the contained liquid moves horizontally and follows the movement of the tank walls (impulsive component), while an additional (mostly vertical) component generates the sloshing motion of the free fluid surface (convective component). The period of the impulsive component is typically found in the range of 0.1–0.3 sec, while the convective component is excited at much longer periods that often exceed 5 sec. Although a rigorous eigenvalue analysis may result in several modes of vibration regarding both the impulsive and the convective component, usually the first impulsive and convective modes are more than enough to capture the response. In that sense, liquid storage tanks can be modelled using a two-degree-of-freedom (2DOF) system, where the two masses (impulsive and convective) are considered decoupled (Calvi and Nascimbene 2011; Malhotra et al. 2000; Priestley et al. 1986).

The geometric and modal characteristics of the hydrodynamic problem are determined using equivalent parameters for the impulsive and convective masses. The two components are distinguished with the aid of subscripts "i" and "c", respectively. According to Veletsos and Tang (1990), it is possible to obtain estimates for the natural periods (T_i and T_c), the masses (m_i and m_c) and the effective heights (h_i and h_c) of each component (see also Malhotra and Veletsos 1994c and Eurocode 8-4, CEN 2006). However, other studies (Malhotra 1997; Vathi et al. 2013) have shown that the contribution of the convective mass to the overall response of the structure can be ignored (especially for non-slender tanks with sufficient freeboard), as the impulsive mass is held responsible for the majority of damage that tanks suffer during earthquakes. The proposed approach similarly decouples the two components, and considers only the impulsive mass to determine the global response, while the effects of the convective sloshing mode are separately estimated. Note that special care should be exercised for liquid storage systems with insufficient freeboard, as part of the convective mass may become impulsive and the terms m_i and m_c should properly be adjusted (Malhotra 2005).

The proposed "Joystick" model

The proposed "Joystick" model consists of a beam-column element that carries the impulsive mass and is supported by fully rigid beam spokes, which in turn rest on point/edge springs (see Fig. 1(a), (b)). An even number of radially distributed rigid beam-spokes forms the base plate as shown in Fig. 1(c). The nonlinear behavior of the system is induced through zero-length edge springs that connect the base plate to the ground. The spring properties refer to a uniform width (b_w) on the base plate

$$b_w = \frac{2\pi R_t}{n}, \tag{1}$$

where 'n' is the number of beams used for the modelling of the base plate (preferably $n\geq 8$), and R_t is the tank radius. An elastic nonlinear material is used to idealize the uplift resistance of the edge springs, while the properties of the elastic element that connects the fluid mass to the base are estimated using the equivalent stiffness that corresponds to the fundamental (impulsive) period and mass. Note that the inelastic nonlinear material (with severe pinching hysteresis probably) would be a more realistic model for the edge springs, in particular for systems that rest on flexible foundation, where negative deformations during unloading can be larger than positive. The proposed tank model and its deflected shape are shown in Fig. 2.

In order to obtain the response of a liquid storage system, a 'pre-analysis' step is necessary to determine the uplift resistance of the supporting edge springs. This step is performed through the analysis of a single base plate strip (Malhotra and Veletsos 1994a), modelled with beam-column elements (Fig. 1(b)). Note that although the 'pre-analysis' step may take a few minutes to complete, only a single run is required to calibrate the actual tank model. Once calibrated, the model is capable to perform nonlinear static or dynamic analysis in seconds, without having to repeat the relatively time-consuming 'pre-analysis' step. Another interesting feature of the model is its ability to simulate not only unanchored but also anchored tanks. In the latter case, the equivalent "edge springs" (Fig. 1(a)) are modified such that their stiffness also takes into account the effect of the bolts that are equally distributed along the perimeter of the base plate (Fig. 3).

Model calibration (pre-analysis)

The *pre-analysis* step requires that the base plate is divided into a number of strips (Fig. 1(c)). A single strip is individually examined to determine its uplift resistance and calibrate the model. The resulting strip model shown in Fig. 1(b) is discretized into a number of force-based fiber beam-column elements, with an approximate element size of $15t_b$, where t_b is the base plate thickness. A uniaxial elastoplastic material is assigned to the fibers, in order to capture the inelastic behavior of the base plate during uplift. Geometric nonlinearities are also taken into account through the co-rotational formulation. Neglecting large-displacement nonlinearities in the response results in what Malhotra and Veletsos (1994a) call the "bending solution", which deviates from the true solution as catenary string effects are ignored. This means that in reality as the edge of the tank is uplifted, the base is not only bent but also tensioned.

A series of Winkler springs is used to model the foundation of the strip model (Fig. 1(b)). The unanchored liquid storage system is assumed to rest on a uniform soil (or concrete) slab layer, thus implying an analogous base/soil stiffness of modulus E_w (e.g. E_w=1.0 GPa for a practically rigid foundation). The Winkler springs are assigned an elastic-no-tension material, suitable for allowing the tension-free uplift of the base plate. As the tank is uplifted, local buckling tends to develop in the vicinity of the (base) plate-wall joint. In order to capture the (base) plate-wall joint stiffness, edge rotational and axial springs are provided, as shown in Fig. 1(b). The stiffness of those springs, for a given width of the strip (b_w) and wall thickness (t_w), is determined following the suggestions found in Malhotra and Veletsos (1994a). $k_{\theta\theta}$ is the rotational and k_{uu} the translational (axial) edge stiffness:

$$k_{\theta\theta} = \frac{E b_w t_w^2 (t_w / R_t)^{1/2}}{2\left[3(1-v^2)\right]^{3/4}} \tag{2}$$

$$k_{uu} = \frac{E b_w (t_w / R_t)^{3/2}}{\left[3(1-v^2)\right]^{1/4}} \tag{3}$$

E is the steel Young's modulus and v the Poisson's ratio. Malhotra and Veletsos (1994a) also suggested a third term, $k_{\theta u}$, that represents the interaction between rotation and translation. However, this term is neglected, as it cannot be incorporated using uniaxial springs. Sensitivity analyses of $k_{\theta\theta}$ and k_{uu} (presented in a latter section) have indicated that such terms do not have a significant effect anyway. Moreover, a concentrated moment (M_r) and an axial force (N_r) are applied on the plate boundary in order to capture the effect of the hydrostatic pressure (p_h) acting on the tank wall. These actions induce some local uplift on a narrow area close to the base plate-wall joint.

$$M_r = \frac{b_w R_t t_w p_h}{2\left[3\left(1-v^2\right)\right]^{1/2}} \tag{4}$$

$$N_r = \frac{b_w \sqrt{R_t t_w}\, p_h}{2\left[3\left(1-v^2\right)\right]^{1/4}} \tag{5}$$

Anchorage

Appropriate modifications are necessary to model anchored liquid storage tanks. Anchorage is introduced to the "Joystick" model through additional vertically-oriented uniaxial springs, one at the end of each beam-spoke. Each spring is assumed to carry a number of bolts that are equally distributed along the width b_w, as shown in Fig. 3 (see also Fig. 1(c), Eq. (1)). Assuming that rigid steel flanges connect the anchors to the tank wall, the stiffness may be calculated as

$$K_b = \frac{EA_b}{L_b}, \tag{6}$$

where A_b is the total area of the bolts and L_b their respective length. The anchoring springs are thus located on the circumference of the base plate and are introduced to the model through an elastoplastic, no-compression, uniaxial force-displacement relationship. A more faithful representation of the anchors may be achieved: (a) by adding an ultimate displacement δ_u to indicate fracture of the bolted connection and (b) by using a damageable "gap" material for the springs. The latter offers the ability to accumulate damage on the yielding anchors in the form of permanent elongation that causes a characteristic displacement gap before tension is developed in reloading (McKenna and Fenves 2001).

Engineering Demand Parameters

Having such a simple model at our disposal, the failure modes that it is able to capture must be identified. Field investigations after major earthquakes have revealed a variety of failure modes on atmospheric tanks. The most common types of failure are shell buckling, sloshing damage to the upper tank shell and roof, and base sliding. Note that the latter is not necessarily a failure unless it results in pipe rupture, as limited sliding could be beneficial due to the flexibility and damping it provides).

During strong ground motion events, hydrostatic and hydrodynamic effects may lead to high internal pressure on the tank walls. Overturning for those thin-walled shell structures is resisted by axial compressive stresses in the wall. Even though high pressure may increase the capacity against buckling, local yielding may trigger an elastic-plastic buckling failure around the lower course of the tank's perimeter, known as the "Elephant's Foot Buckling" (EFB). When partial uplift is allowed, either due to absence of anchorage or due to poor detailing of the anchors, the rotation of the plastic hinge in the tank base should not exceed a certain rotational capacity, specified in modern codes (e.g. API-650, American Petroleum Institute 2007 and Eurocode 8-4, CEN 2006). Moreover, the excitation of the long period convective mode may cause sloshing of the contained liquid, which may in turn damage the upper parts of the tank (roof, upper course).

EFB can be captured by comparing the compressive meridional stress against a critical limit such as the formula proposed by Rotter (2006). The EFB stress limit is compared to the corresponding stress estimated through the axial edge spring force recorded during the analysis. The latter implies that the stress estimation is highly connected to the number of edge springs found on the tank circumference. A fine discretization on the base plate in terms of beam-spokes may allow for a more accurate stress distribution on the edge to be considered. Alternatively, a concentration factor could be applied on a less refined base plate model to take into account the actual stress distribution locally.

As far as plastic rotation is concerned, one may employ direct measurements through the fiber sections adopted for the base plate strips. Alternatively, the direct mapping between uplift (w), separation length (L) and plastic rotation (θ_{pl}) suggested by Eurocode 8-4 (CEN 2006) could be adopted

$$\theta_{pl} = \frac{2w}{L} - \frac{w}{2R_t}, \tag{7}$$

which also indicates that the response is closely related to the uplift mechanism of the tank. Viscous damping selected for the model is purely associated with the impulsive mode. Malhotra (1997) suggests different values of impulsive mode damping appropriate for each failure mode, akin to an equivalent approach to account for hysteresis among other issues. Since a single model is only used in our approach to convey all such information at once, a single value of damping (e.g. 2% according to Malhotra (2000) and Eurocode 8-4 (CEN 2006)) is recommended.

The sloshing response may be incorporated by adding the convective mass to the model (similarly to the impulsive component) or alternatively, by ignoring uplift altogether and using the spectral acceleration at the convective mode period only to estimate the wave height according to formulas provided by design codes. For example, $d_{API\text{-}650}$ and d_{EC8} are the maximum sloshing wave height estimates according to API-650 (American Petroleum Institute 2007) and Eurocode 8-4 (CEN 2006) respectively:

$$d_{API-650} = R_t A_f \tag{8}$$

$$d_{EC8} = R_t \frac{0.84 S_a(T_{c1}, 0.5\%)}{g} \tag{9}$$

A_f is the acceleration coefficient for sloshing wave height calculation and $S_a(T_{c1},0.5\%)$ the elastic response spectral acceleration at the 1st convective mode of the fluid for a damping value equal to 0.5%.

Numerical Example

Detailed Finite Element Model

In order to validate the uplifting mechanism of the proposed model, a comparison is performed against detailed 3D finite element models for three unanchored tanks of varying geometry and aspect ratio (h_f/R_t). Complex hydrodynamics and fluid-structure-interaction are not tackled. Instead, such effects are taken into account through the Veletsos and Tang (1990) impulsive pressure distribution that is also adopted by Malhotra and Veletsos (1994c) and Eurocode 8-4 (CEN 2006). Bound on this approximation, the performance of the proposed model is assessed versus detailed finite element models with respect to the base plate uplifting mechanism.

The geometric and material characteristics of the tanks are summarized in Table 1. The analyses are performed using the general-purpose FE code ABAQUS (2011). Fig. 4 presents a typical mesh of the systems considered, where the unanchored tank rests on a fully rigid surface. The base plate and the rigid surface form a contact pair that is assigned appropriate interaction properties such that uplift is allowed. The rigid surface is modelled using 4-node rigid quadrilateral elements (R3D4), and the tank shell using 4-node reduced integration shell elements (S4R). Special attention is paid to the annular plate as well as to the lower courses of the tank, where modes of failure similar to uplift and EFB are expected to occur. Note that the roof of the tank is not explicitly modelled. Instead, a rigid body constraint is assigned to the upper course top nodes. Although one may argue that the flexibility of the supporting truss of the roof shell could modify the response, this effect can be considered negligible for fixed (non-floating) roof tanks, which is consistent with the assumptions of Malhotra and Veletsos (1994c).

A nonlinear static analysis is conducted in three stages. Fig. 5 illustrates the loading sequence during the analysis. Gravity loads are initially applied to the "empty" (i.e. zero hydrostatic loads) tank such that contact is established with the rigid surface. Once the tank has settled on the ground, hydrostatic loads are applied on the walls and the base plate of the system. The initial conditions imposed by hydrostatic pressure are followed by the hydrodynamic loading, the distribution of which is obtained through the impulsive pressure equation (Veletsos and Tang 1990):

$$p_i(\xi,\zeta,\varphi,t) = C_i(\xi,\zeta)\rho_f h_f \cos(\varphi) A(t) \tag{10}$$

C_i is a spatial function for the non-dimensional cylindrical coordinates ξ, ζ, φ (with origin at the center of the tank bottom and ζ being the vertical axis) and $A(t)$ the impulsive mass response history acceleration. Fig. 6 presents a comparison between the "Joystick" model and the detailed FE model shown in Fig. 4, for a constant input acceleration of $A(t)$=1.0g and the tank parameters of Table 1. The deformability of the model is examined in terms of base uplift (w) versus the separation length (L). A very good agreement is observed for tank A, while small discrepancies are evident for tanks B and C. In particular, for a given uplift of tank B the "Joystick" model underestimates the separation length compared to the FE model, thus implying a slightly stiffer behavior. In that sense, the response seems to be overestimated for low aspect ratio liquid storage systems similar to tank B by a factor roughly equal to 0.3. Although this kind of difference is borderline acceptable for a simplified model, it occurs following the onset of the Elephant's Foot Buckling where the tank has "failed", and as a result, the edge support conditions on the base are no longer valid. For a slender system such as tank C, the response is clearly underestimated. Initially the factor between the two curves is in the order of 0.15, but as the base uplift approaches the rather large value of 140mm it comes very close to 0.3. Note that the inherent error in the simplifications adopted by Malhotra and Veletsos (1994c) that also appears in the finite element model (e.g. approximate hydrodynamic loading in place of fluid-structure-interaction, Fig. 5), should also be considered following relevant experimental studies (De Angelis et al. 2009; Ormeño et al. 2015). In a true performance-based sense, this error (although only roughly estimated) should also be acknowledged in the accuracy of results in terms of model-related uncertainty.

Performance of the proposed model

The application of the proposed model is presented for the squat tank A that has a radius of R_t=13.9m and is 95% filled with water (Table 1). An overview of the strip model response is initially presented through the uplift resistance and plastic rotation plots shown in Fig. 7. According to Fig. 7(a), the strip model yields by the time some minor uplift is induced. As the model is further uplifted, stiffness degradation takes place and the response becomes essentially elastoplastic with constant hardening. Fig. 7(b) compares the recorded model plastic rotation and the corresponding estimate of Eq.(7). Apparently, the Eurocode 8-4 (CEN 2006) approximation of the plastic rotation seems to saturate for uplift values greater than 5cm. Thankfully, it presents a conservative approximation compared to the estimates of the proposed model, where the maximum difference between the two curves is in the order of 15%.

The base plate rotational response is shown in Fig. 8. Again, the response is dominated by a very stiff elastic branch that yields when uplift takes place and is then followed by a hardening behavior, similar to the one observed on the strip model analysis results. The response pattern does not change for the full tank model either, where results are provided both for anchored and unanchored support conditions. Although it is customary to assume fixed boundary conditions for the modelling of anchored tanks, the "Joystick" model provides a more elaborate solution by taking into account the anchorage effect, which according to post-earthquake observations by no means implies zero uplift.

A parametric study is conducted using a range of ultimate displacements for the anchored connections, in order to obtain a deeper understanding on the response of anchored systems. The nonlinear static as well as the time history analysis are employed for ultimate displacement values ranging from δ_u =1cm to δ_u =20cm. This range for δ_u is meant to reflect the potential flexibility of the entire connection, including the bolt and the connecting flange. The results presented in Fig. 9 show the edge uplift versus the horizontal force that is incrementally applied on the impulsive mass of the tank model. It is evident that the bolts shift the yield point to considerably higher base shear estimates, until the anchors begin to fail and the response of the anchored system changes. A progressive fracture of the connections (followed by a sudden drop of the system's stiffness) takes place, spoke after spoke, until the response becomes similar to that of the unanchored tank. Fig. 10 and Fig. 11 present the uplift and rotation histories, respectively, for a scaled version of the El-Centro record; they fully capture the rocking motion of the tank, while at the same time, the effect of the anchors' ultimate displacement is unveiled during the first 10 seconds of the ground motion. Once again, the bolt connections restrain the system until the progressive failure of the anchors takes place and the response gradually matches that of the unanchored tank.

Influence of Modelling Parameters

Fig. 12 compares various modelling choices in terms of discretization (mesh) and element type (displacement versus force-based distributed plasticity) used for the strip model 'pre-analysis' step. The displacement-based formulation presents a slightly stiffer response compared to the corresponding force-based solution for an element size not greater than $20t_b$. When the discretization is further refined, both formulations exhibit practically identical response. Apparently, at the optimal discretization level in terms of accuracy (i.e. $15t_b$), either can be used bearing in mind that the displacement-based approach is considerably faster. In general, the strip model mesh seems to yield an accurate solution at an element size of approximately $10t_b$-$15t_b$. As an alternative, only the outer quarter of the strip model could be assigned a fine mesh (in the order of $15t_b$), in the sense that the plastic hinges are unlikely to form outside this given range. The remaining three quarters may then be modelled using an element size of the order of $45t_b$ to further improve the computational time.

Sensitivity Analysis

Besides the model type uncertainty outlined in the previous sections of this paper, a thorough performance-based approach for practically any earthquake engineering problem should take into account sources of uncertainty such as the model parameter uncertainty, the record-to-record variability and the seismic hazard uncertainty. In this section a sensitivity analysis is conducted in order to determine the effect of different input parameters on the seismic response of the model (i.e model parameter uncertainty). Tank A (Table 1) is used as a testbed. Key-parameters such as the steel elastic Young's modulus (E) and the expected yield strength (f_y) are examined. Other geometric parameters examined are: the tank wall thickness (t_w), the annular ring thickness (t_a) and the base plate thickness (t_b) and the contained fluid height (h_f). The edge rotational ($k_{\theta\theta}$) and axial springs (k_{uu}) suggested by Malhotra and Veletsos (1994a) are also considered as potential sources of modelling uncertainty and hence both parameters are included in the sensitivity analysis through a stiffness modification factor (α_k). Finally, the bolts' yield strength (f_b) is included for the case of anchored systems. The aforementioned parameters are summarized in Table 2, where the coefficients of variation (CoV) adopted (following either Vrouwenvelder 1997, or engineering judgement) are used to provide upper and lower bound estimates for the majority of variables.

Sensitivity analysis with respect to nonlinear static (Pushover) and dynamic (Incremental Dynamic Analysis, IDA (Vamvatsikos and Cornell 2002)) analysis are performed. A set of three nonlinear static analyses is performed for each parameter, corresponding to the response when parameters are assigned their mean, upper and lower bound values. Having eliminated the modelling parameters that the structure has shown small sensitivity to, IDA is performed to provide further insight by taking into account the record-to-record variability. Although it is not presented herein, the effect of the site can be incorporated at a later stage via convolution with the seismic hazard.

Nonlinear Static Analysis sensitivity

Fig. 13 presents the modelling sensitivity in terms of nonlinear static curves for the parameters of Table 2. The sensitivity to material uncertainty (E, f_y) is shown in Fig. 13(a) and (b). It is evident that the material properties are of minor importance as both the upper and the lower bound curves are perfectly aligned to the mean estimates. Other parameters, such as the strip model edge springs, are also strongly related to modelling associated uncertainty. The sensitivity analysis for both rotational and axial edge springs is presented in Fig. 13(c) and (d) respectively. Although the model is not sensitive to the rotational spring, the axial component affects the response for large uplift deformations (e.g. 0.20m of uplift).

The geometric characteristics comprise another potential source of uncertainty, especially for the case of liquid storage tanks, where loss of material subject to sulfide or seawater corrosion, construction quality and mid-life rehabilitation interventions (typically every 12 years) determine the effective tank wall and base plate thickness. According to Fig. 13(e), the base plate thickness does not cause any significant change in the response for the given range. The annular ring thickness on the other hand is significant, due to the post-yield response modification shown in Fig. 13(f). Decreasing t_a reduces the strength of the tank. At the same time, when t_a exceeds its mean value the response becomes stiffer and the plastic hinge formation on the base plate shifts to slightly higher base shear estimates. In general, the base plate thickness modifies the post-yield behavior of the model for uplift values no greater than 0.25m. One may notice the significance of the annular ring over the base plate thickness, as the former determines response in the critical plastic hinge position. Still, there cannot be a solid prediction regarding the importance of base plate thickness, as the governing parameter is a function of the annular ring (radial) width. For typical design specifications for the annular ring (e.g. American Petroleum Institute 2007), the plastic hinge will form within its width. For the rare case where such specifications are not respected and an insufficiently wide ring is provided, the hinge will form within the base plate and t_b rather than t_a will govern the response. Apart from the base plate properties, the tank wall sensitivity shown in Fig. 13(g) does not considerably affect the response, except for large uplifts where minor changes take place on the nonlinear static curves.

The contained liquid height shown in Fig. 13(h) summarizes the geometric properties evaluation. The fluid height given as a fraction of the total height of the tank, is by far the most influential parameter examined, as the discrepancies found between the $0.50h_t$ and the $0.99h_t$ curves, for a given uplift, are in the order of 35% following the plastic hinge formation. Reducing the fluid stored in the tank results in stiffer models, while as it approaches the maximum storage capacity, the system's strength is significantly reduced, resulting into a more vulnerable structural system. Finally, for the case of anchored tanks, the bolts' yield strength is also examined, where according to Fig. 13(i) the effect can be considered negligible, in contrast to the significant sensitivity shown for the connection ductility in Fig. 9.

IDA sensitivity

The nonlinear static analysis results have shown that the most influential parameters are the fluid height, the tank wall thickness, the annular ring thickness and the stiffness of the axial spring. A series of IDAs is performed for these parameters in order to validate the static analysis results. A set of 22 pairs of far-field records (FEMA 2009) is used. The uplift is adopted as the engineering demand parameter (*EDP*) and the peak ground acceleration (*PGA*) as the intensity measure (*IM*). Other *EDPs* are functionally one-to-one related to uplift through the 'pre-analysis' step, hence any conclusions drawn for uplift are also applicable. Regarding the *IM* considered, although *PGA* is expected to inflate the final output of a seismic risk assessment study with additional uncertainty (i.e. it is not the optimal intensity measure), it is intentionally adopted herein in order to make the sensitivity analysis results easier to digest even for readers that are not familiar with terms such as efficiency and sufficiency (Luco and Cornell 2007). In any case, given that there is no obvious optimal intensity measure for the global response of the tank (as the convective spectral acceleration would be for the sloshing wave height for instance), the effect of the parameters examined is not expected to change significantly using any other intensity measure. Either way, when the period falls within a range of 0.1-0.3sec, such as the case of the tanks examined, *PGA* and the fundamental period spectral acceleration provide very similar results. Undeniably, more *IM* options could be tested in order to find the optimal *IM* (e.g. the spectral acceleration at some elongated period for unanchored tanks). However, this is beyond the scope of this study and is expected to be covered in a future direction of our research.

Fig. 14 presents the median IDA sensitivities. It is evident that geometric parameters such as the tank wall (Fig. 14(a)) and the annular ring thickness (Fig. 14(b)) do not introduce any significant demand uncertainty to our model (although the associated capacity may indeed change), as all curves are almost perfectly aligned to each other. The same observation applies for nearly the entire given uplift range of the axial spring stiffness (Fig. 14(c)). One may notice that the lower bound deviates from the mean estimate for uplift values greater than 0.22m, yet the difference may be considered statistically insignificant.

Fig. 14(d) shows that the fluid height introduces a considerable level of uncertainty to the model. Even though the median IDA curves follow the exact same pattern with the nonlinear static analysis results for a fluid height up to 75% of the tank height, it appears that as the fluid height increases, the response changes considerably. The $0.80h_t$ curve coincides with the $0.75h_t$ curve, while both the $0.90h_t$ and the $0.99h_t$ curves develop a substantially stiffer response for peak ground accelerations that exceed 0.1g. The performance obtained summarizes the fluid height uncertainty involved in liquid storage tanks. The paradox of having a more massive (and hence flexible) system (i.e. $0.99h_t$ curve) oscillating at smaller uplifts for a given *IM* level compared to the $0.75h_t$ case, may be attributed to the period effect shown in the Fig. 15 median spectrum. It appears that as the liquid stored in the tank increases, the impulsive period elongates. Initially, this brings T_i within the ascending branch of the median spectrum and as a result the impulsive spectral acceleration ($S_a(T_i)$) increases too. After the $0.8h_t$ impulsive period (Fig. 15(b)), a decrease on the median spectral acceleration (for given *PGA*) is observed instead.

Conclusions

A novel modelling approach has been presented for the rapid analysis of liquid storage tanks. The proposed model offers reasonable accuracy and good computational efficiency compared to detailed FE models. Based on the principles of Malhotra and Veletsos, the proposed model goes one step beyond by providing the ability for three-dimensional analysis of liquid storage systems using multiple ground motion components. It can easily be applied using any general purpose structural analysis software, thus taking advantage of the abilities offered by commercial codes. It is a simplified model suitable for practically any cylindrical fixed-roof liquid storage system, regardless of geometry, material and boundary conditions. The motivation behind this methodology is the need for probabilistic assessment, where numerous scenarios using nonlinear static or dynamic analysis are necessary. All in all, the proposed model forms a concept that employs modern tools for the successful performance-based assessment/design of a single liquid storage system, or maybe even an ensemble of tanks.

Acknowledgements

This research has been co-financed by the European Union (European Social Fund – ESF) and Greek national funds through the Operational Program "Education and Lifelong Learning" of the National Strategic Reference Framework (NSRF) - Research Funding Program: THALES. Investing in knowledge society through the European Social Fund.

References

"ABAQUS Documentation (6.11)." (2011). Dassault Systèmes, Providence, RI, USA.

Ahari, M. N., Eshghi, S., and Ashtiany, M. G. (2009). "The tapered beam model for bottom plate uplift analysis of unanchored cylindrical steel storage tanks." *Engineering Structures*, Elsevier Ltd, 31(3), 623–632.

American Petroleum Institute. (2007). *Seismic Design of Storage Tanks - Appendix E, Welded Steel Tanks for Oil Storage*. API 650, 11th Edition, Washington, D.C.

De Angelis, M., Giannini, R., and Paolacci, F. (2009). "Experimental investigation on the seismic response of a steel liquid storage tank equipped with floating roof by shaking table tests." *Earthquake Engineering & Structural Dynamics*, 39(4), 377–396.

Buratti, N., and Tavano, M. (2014). "Dynamic buckling and seismic fragility of anchored steel tanks by the added mass method." *Earthquake Engineering & Structural Dynamics*, 43(1), 1–21.

Calvi, G. M., and Nascimbene, R. (2011). "Progettazione sismica dei serbatoi." *Progettare i gusci*, IUSS Press, 537–672.

CEN. (2006). *Eurocode 8: Design of structures for earthquake resistance–Part 4: Silos, tanks and pipelines*. *European Committee for Standard*, Brussels.

Cortes, G., Prinz, G. S., Nussbaumer, A., and Koller, M. G. (2012). "Cyclic Demand at the Shell-Bottom Connection of Unanchored Steel Tanks." *Proc., 15th World Conference on Earthquake Engineering*, Lisboa, Portugal.

FEMA. (2009). *Quantification of Building Seismic Performance Factors*. FEMA P-695, prepared by Applied Technology Council for Federal Emergency Management Agency, Washington, D.C.

Girgin, S. (2011). "The natech events during the 17 August 1999 Kocaeli earthquake: Aftermath and lessons learned." *Natural Hazards and Earth System Science*, 11(4), 1129–1140.

Hatayama, K. (2015). "Damage to Oil Storage Tanks due to Tsunami of the Mw9.0 2011 off the Pacific Coast of Tohoku, Japan Earthquake." *Earthquake Spectra*, 31(May), 1103–1124.

Kilic, S., and Ozdemir, Z. (2007). "Simulation of Sloshing Effects in Cylindrical Containers under Seismic Loading." *Proc., 6th LS-DYNA Anwenderforum*, Frankenthal.

Luco, N., and Cornell, C. A. (2007). "Structure-Specific Scalar Intensity Measures for Near-Source and Ordinary Earthquake Ground Motions." *Earthquake Spectra*, 23(2), 357–392.

Malhotra, P. K. (1997). "Seismic Response of Soil-Supported Unanchored Liquid-Storage Tanks." *Journal of Structural Engineering*, 123(4), 440–450.

Malhotra, P. K. (2000). "Practical Nonlinear Seismic Analysis of Tanks." *Earthquake Spectra*, 16(2), 473–492.

Malhotra, P. K. (2005). "Sloshing Loads in Liquid-Storage Tanks with Insufficient Freeboard." *Earthquake Spectra*, 21(4), 1185–1192.

Malhotra, P. K., and Veletsos, A. S. (1994a). "Beam Model for Base-Uplifting Analysis of Cylindrical Tanks." *Journal of Structural Engineering*, 120(12), 3471–3488.

Malhotra, P. K., and Veletsos, A. S. (1994b). "Uplifting Analysis of Base Plates in Cylindrical Tanks." *Journal of Structural Engineering*, 120(12), 3489–3505.

Malhotra, P. K., and Veletsos, A. S. (1994c). “Uplifting Response of Unanchored Liquid-Storage Tanks.” *Journal of Structural Engineering*, 120(12), 3525–3547.

Malhotra, P. K., Wenk, T., and Wieland, M. (2000). “Simple Procedure for Seismic Analysis of Liquid-Storage Tanks.” *Structural Engineering International*, 10(3), 197–201.

McKenna, F., and Fenves, G. L. (2001). “The OpenSees Command Language Manual (1.2 edn).”

Ormeño, M., Larkin, T., and Chouw, N. (2015). “The effect of seismic uplift on the shell stresses of liquid-storage tanks.” *Earthquake Engineering & Structural Dynamics*, 44(12), 1979–1996.

Priestley, M. J. N., Wood, J. H., and Davidson, B. J. (1986). “Seismic Design of Storage Tanks.” *Bulletin of the New Zealand Society for Earthquake Engineering*, 19(4), 272–284.

Rotter, J. M. (2006). “Elephant’s foot buckling in pressurised cylindrical shells.” *Stahlbau*, 75(9), 742–747.

Talaslidis, D. G., Manolis, G. D., Paraskevopoulos, E., Panagiotopoulos, C., Pelekasis, N., and Tsamopoulos, J. (2004). “Risk analysis of industrial structures under extreme transient loads.” *Soil Dynamics and Earthquake Engineering*, 24(6), 435–448.

Vamvatsikos, D., and Cornell, C. A. (2002). “Incremental dynamic analysis.” *Earthquake Engineering & Structural Dynamics*, 31(3), 491–514.

Vathi, M., Pappa, P., and Karamanos, S. A. (2013). “Seismic Response of Unanchored Liquid Storage Tanks.” *Proc., ASME 2013 Pressure Vessels & Piping Division Conference*, Paris, France.

Veletsos, A. S., and Tang, Y. (1990). “Soil-structure interaction effects for laterally excited liquid storage tanks.” *Earthquake Engineering and Structural Dynamics*, 19(August 1989), 473–496.

Virella, J. C., Godoy, L. a., and Suárez, L. E. (2006). “Dynamic buckling of anchored steel tanks subjected to horizontal earthquake excitation.” *Journal of Constructional Steel Research*, 62(6), 521–531.

Vrouwenvelder, T. (1997). “The JCSS probabilistic model code.” *Structural Safety*, 19(3), 245–251.

Table 1. Properties of the tanks examined.

Properties	Variable description	Notation (units)	Numerical values		
			Tank A	Tank B	Tank C
Tank	Radius	R_t (m)	13.9	23.47	6.1
	Height	h_t (m)	16.5	19.95	11.3
	Wall thickness per course	t_w (mm)	17.7/15.7/13.7/11.7/9.7/ 7.8/6.4/6.4/6.4	22.23/18.93/16.24/13.57 /10.9/8.22/8.0/8.0/8.0	9.6/8.0/6.4/4.8
	Base plate thickness	t_b (mm)	6.4	6.4	4.8
	Annular ring thickness	t_a (mm)	8.0	10.0	4.8
	Roof mass	m_r (ton)	35	46	19
Material	Yield strength	f_y (MPa)	235	235	235
	Steel Young's Modulus	E (GPa)	210	210	210
	Hardening ratio	a_h (%)	1	1	1
	Poisson's ratio	v (-)	0.3	0.3	0.3
Fluid	Height	h_f (m)	15.7	18.95	11.3
	Density	ρ_f (kg/m^3)	1000	1000	1000

Table 2. Parameters considered for the sensitivity analysis of the proposed model.

Parameter	Notation (units)	Mean (μ) Expected Values	Values Considered
Young's modulus	E (GPa)	210	216.3/203.7
Yield stress	f_y (MPa)	280	299.6/260.4
Edge-spring stiffness factor	a_k	1.0	1.3/0.7
Bolts' strength	f_b (MPa)	900	963/837
Equivalent wall thickness	t_w (mm)	13.1	14.41/11.79
Base plate thickness	t_b (mm)	5.44	6.4/4.48
Annular ring thickness	t_a (mm)	6.8	8.0/5.6
Normalized fluid height	h_f /h_t	0.75	0.5/0.6/0.7/0.75/0.8/0.9/0.99

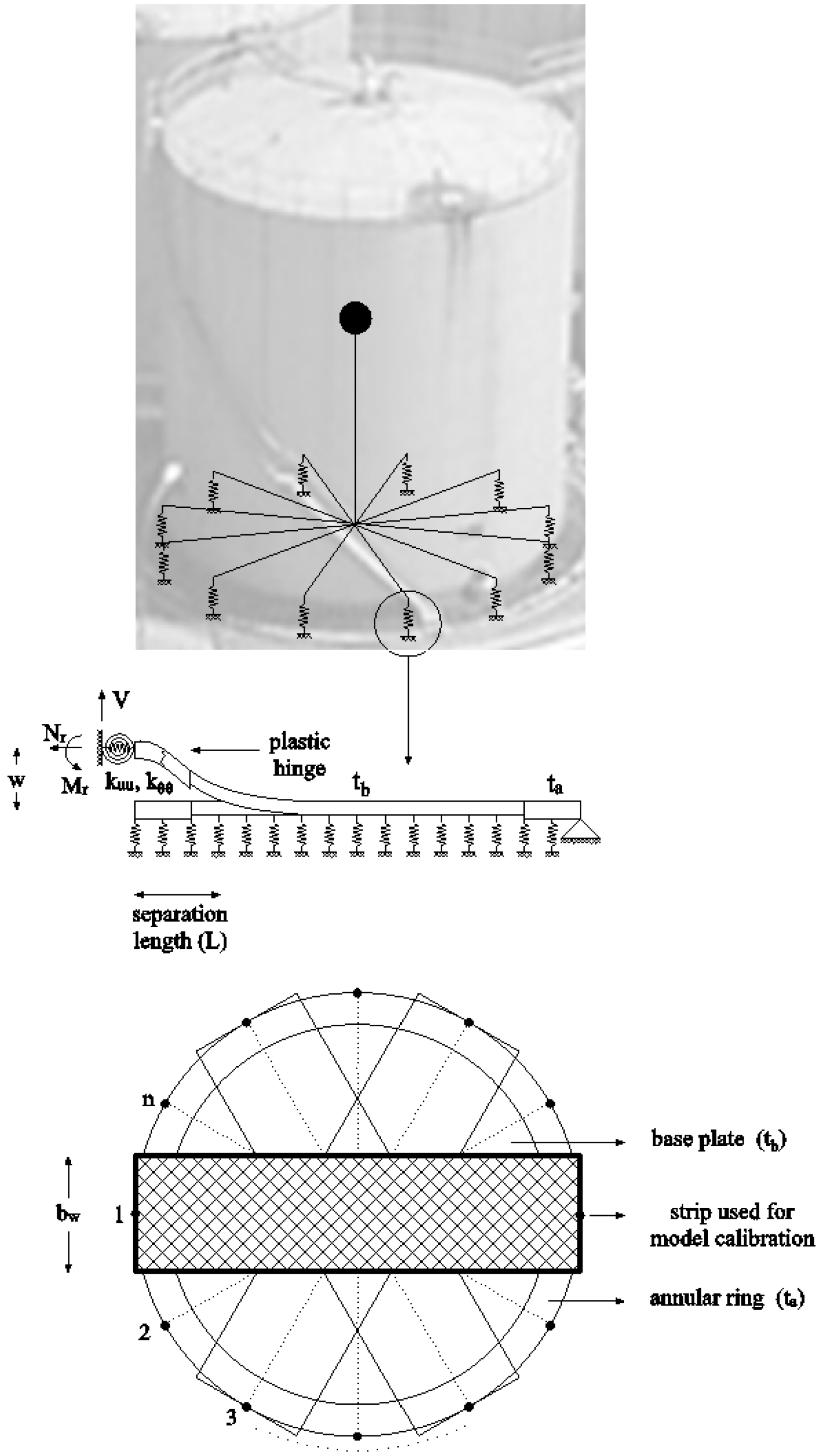

(a)

(b)

(c)

Fig. 1. (a) The "Joystick" model on an actual liquid storage tank. (b) The strip model of the 'pre-analysis' step provides the response of the springs at the edge of each beam-spoke. (c) Base plate discretization, shown for the 'pre-analysis' step. A strip is analyzed to determine the properties of the spring at the end of each spoke.

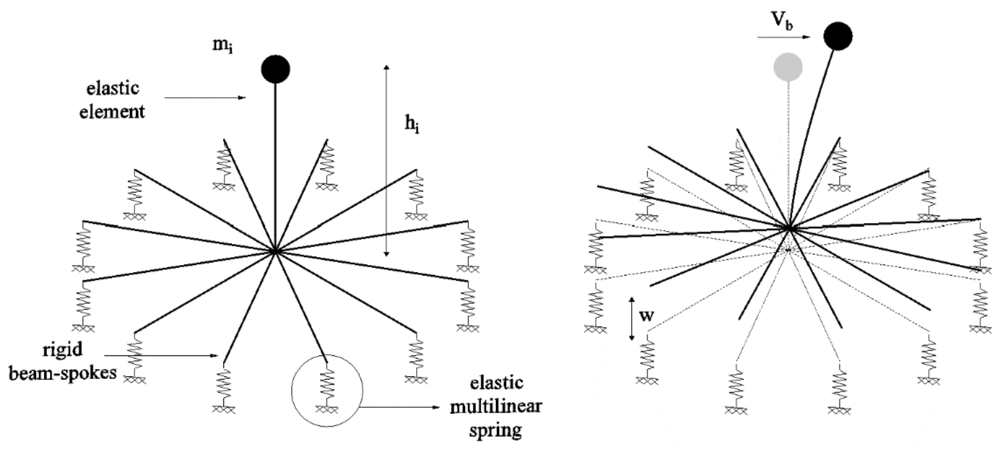

(a) (b)

Fig. 2. (a) The “Joystick” model and (b) its deflected shape.

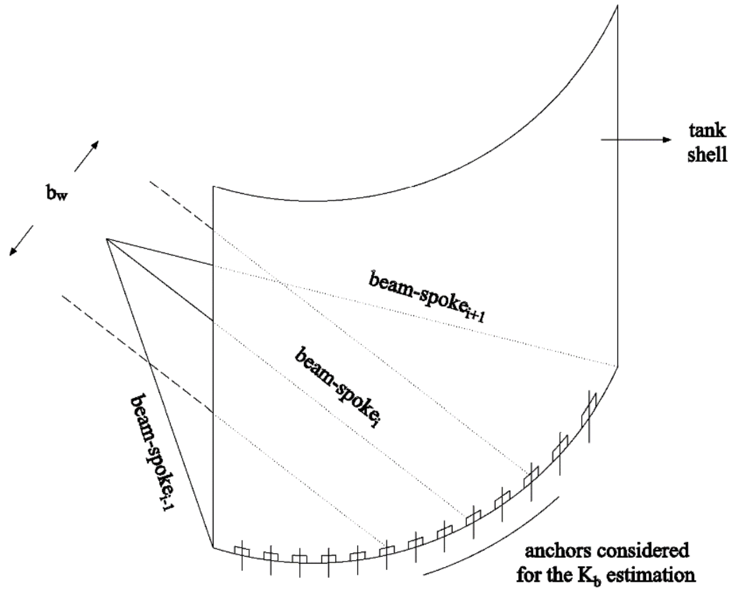

Fig. 3. Part of an anchored liquid storage tank. The rigid beam-spokes of the proposed model are illustrated, featuring the anchors considered for the stiffness estimation shown in Eq.(6).

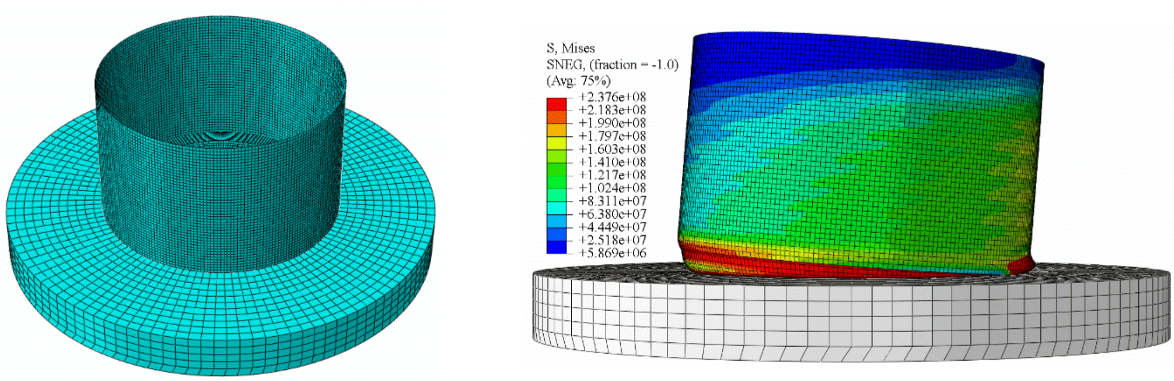

(a) (b)

Fig. 4. (a) Detailed 3D finite element model featuring the contact between the tank and the surrounding rigid surface and (b) von Mises stress contour on the deformed shape of tank A.

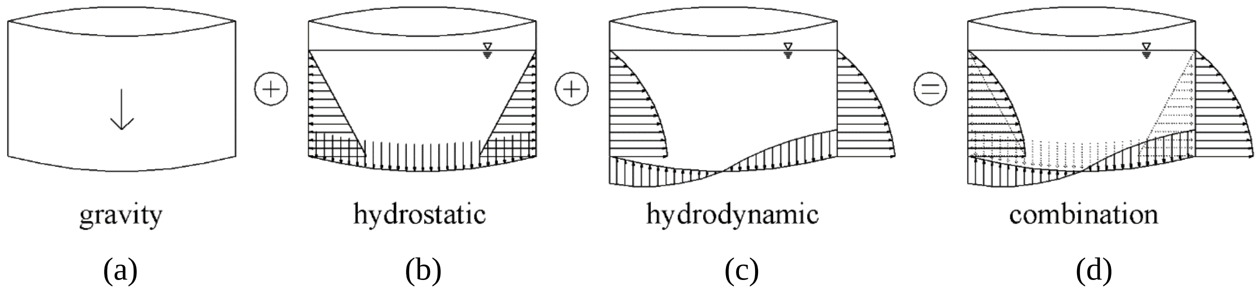

Fig. 5. Loading steps. (a) gravity loads, (b) hydrostatic pressure, (c) hydrodynamic pressure and (d) combined actions.

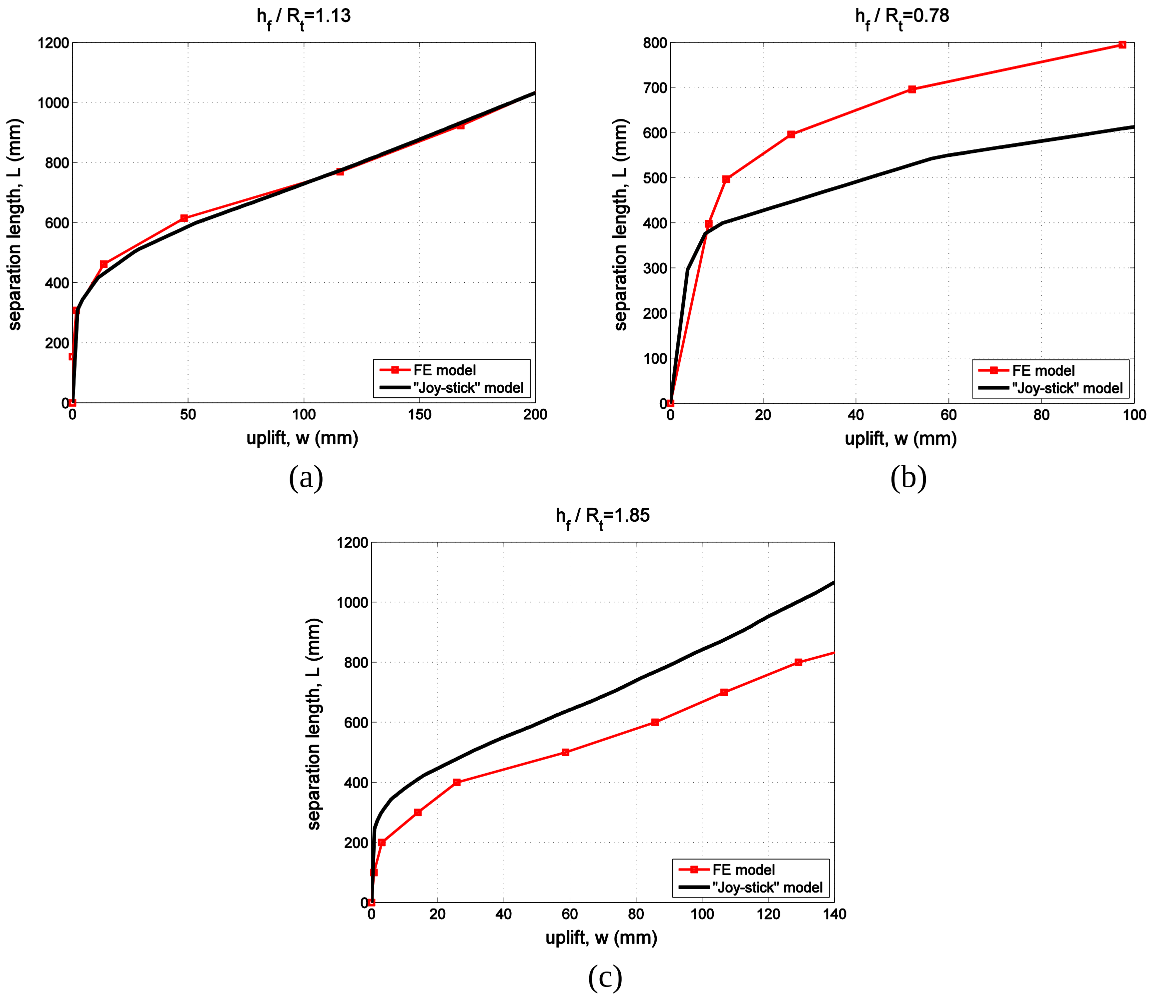

Fig. 6. Separation length versus uplift plots for (a) tank A, (b) tank B and (c) tank C.

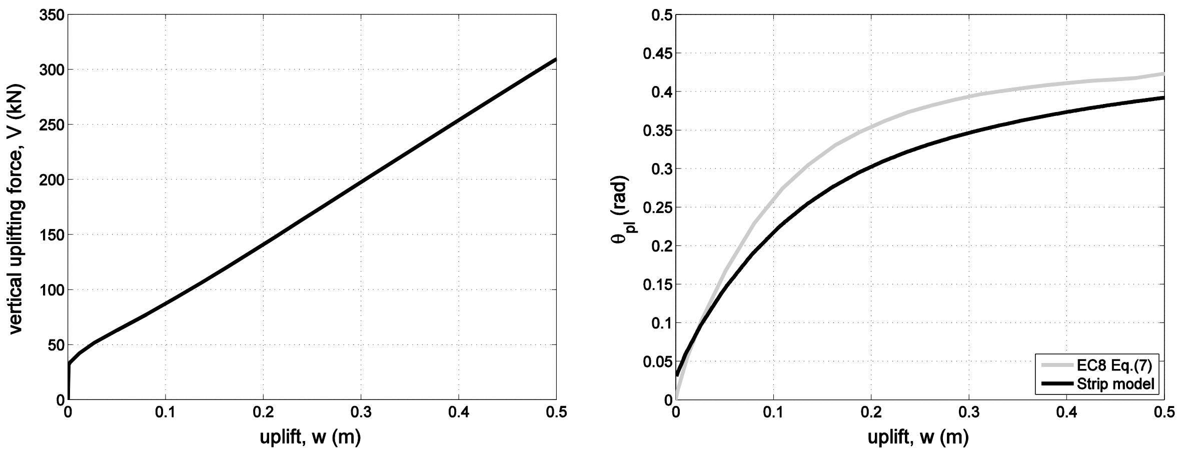

(a) (b)

Fig. 7. (a) Strip model uplift resistance, and (b) edge uplift versus plastic rotation (strip model versus Eurocode 8 prediction).

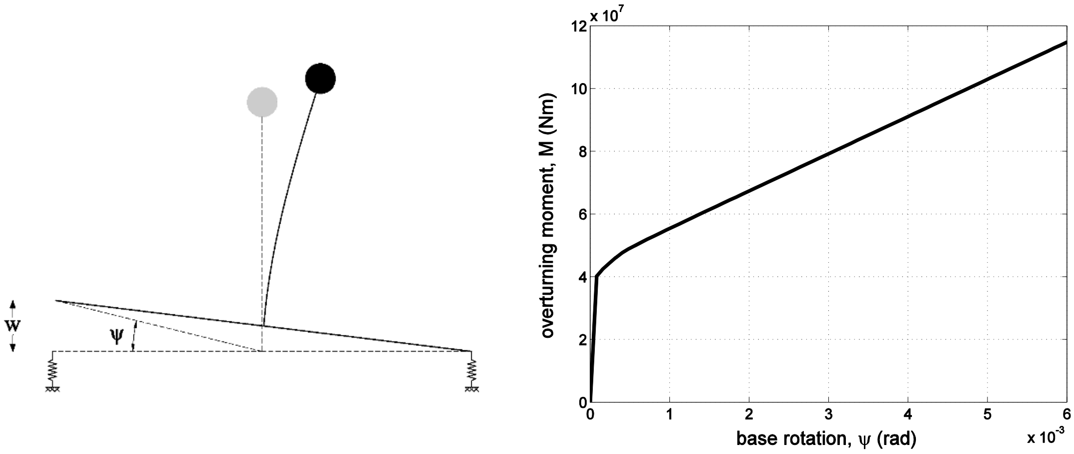

(a) (b)

Fig. 8. (a) Recorded base rotation ψ and (b) base plate rotational resistance.

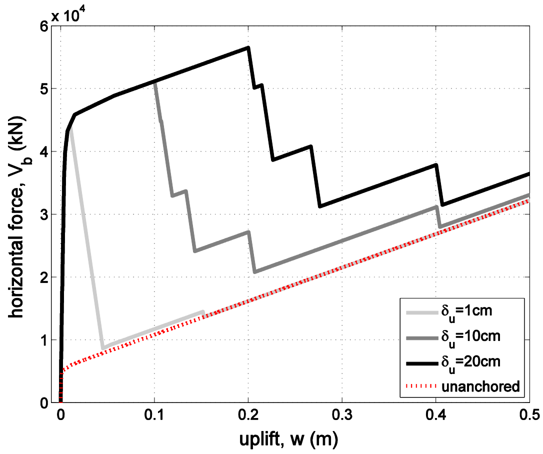

Fig. 9. Nonlinear static analysis. Edge uplift versus horizontal force for a range of ultimate connection displacements (δ_u).

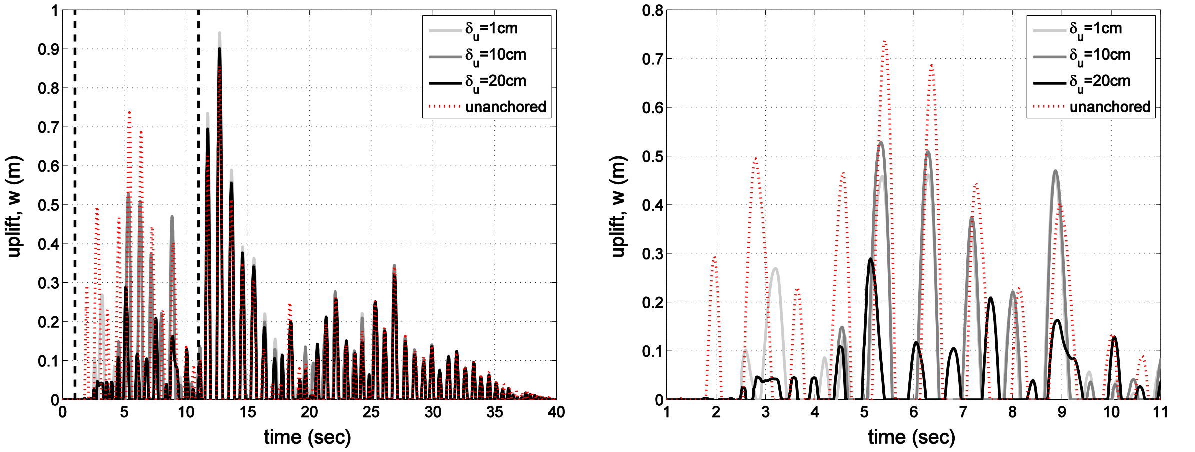

(a) (b)

Fig. 10. (a) Uplift response history and (b) magnified view at 1÷11 sec featuring the effect of anchors.

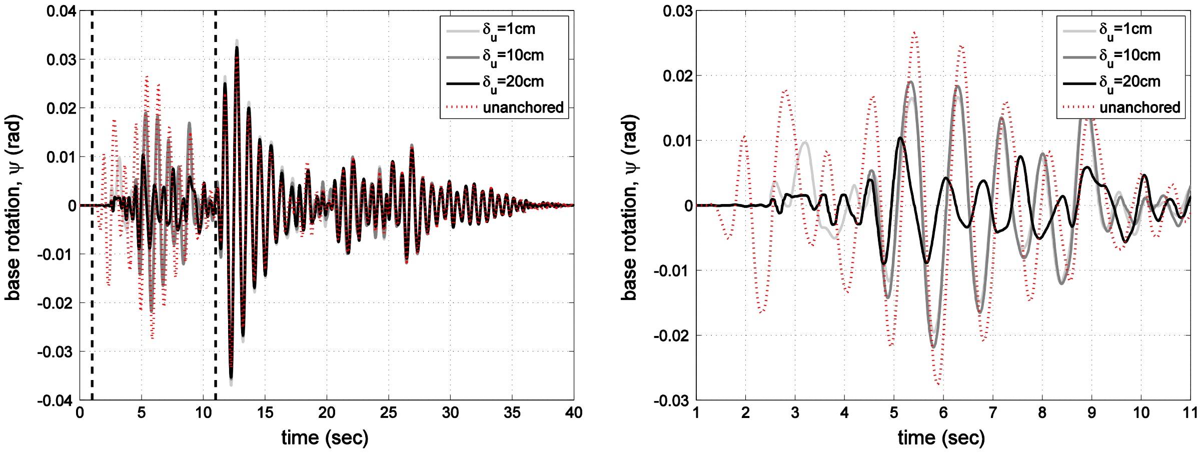

(a) (b)

Fig. 11. (a) Rotational response history and (b) magnified view at 1÷11 sec featuring the effect of anchors.

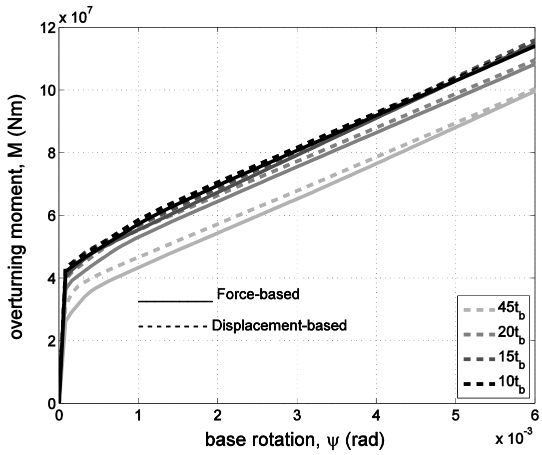

Fig. 12. Parametric base plate nonlinear static analysis on the element size and the beam element formulation.

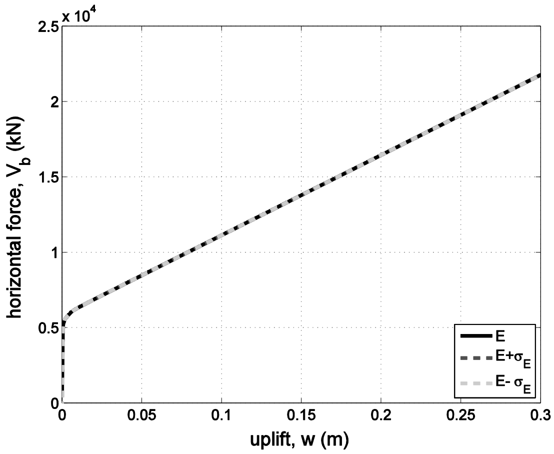

(a) E is of minor importance

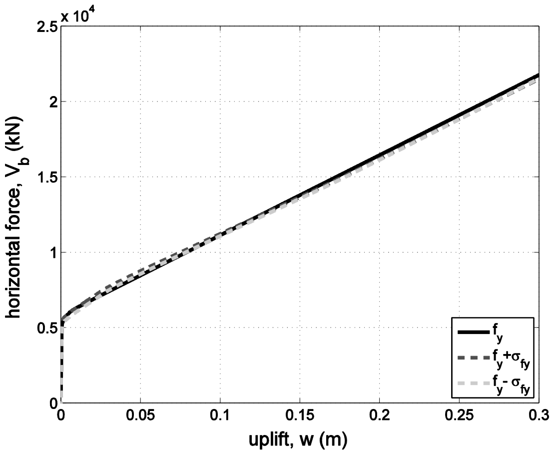

(b) f_y is of minor importance

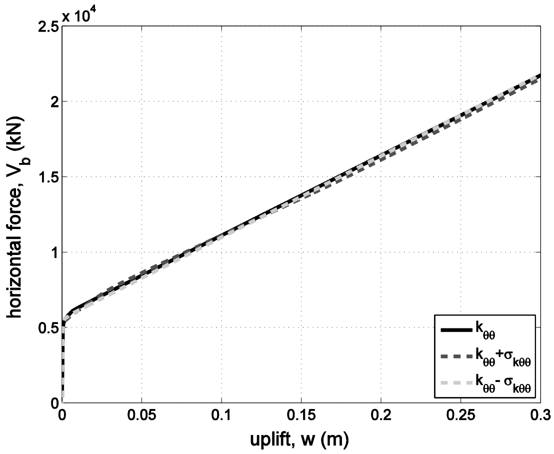

(c) $k_{\theta\theta}$ is of minor importance

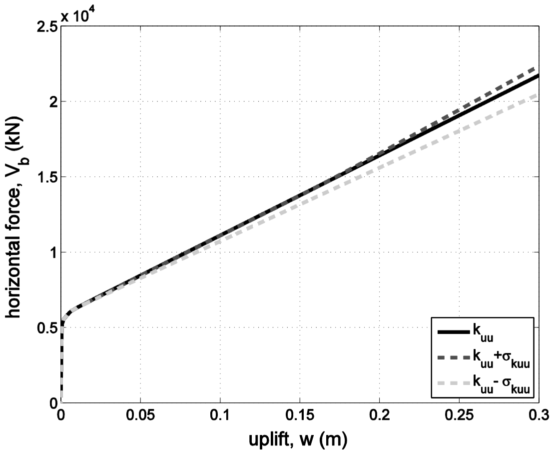

(d) k_{uu} is important for large uplifts

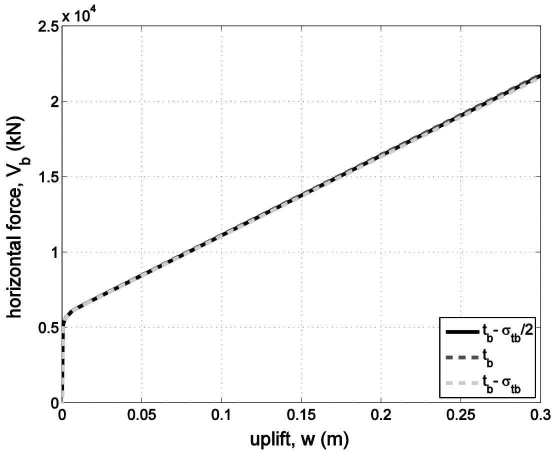

(e) t_b is of minor importance

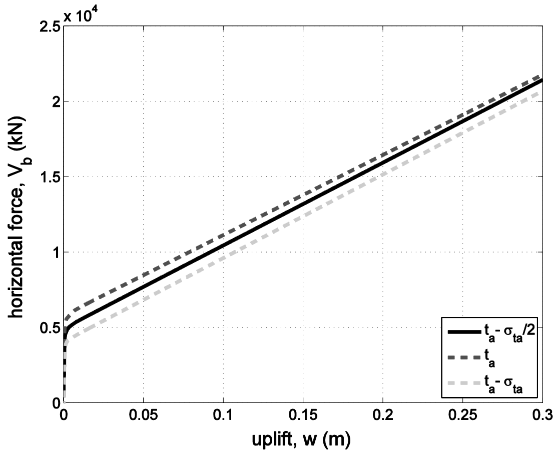

(f) t_a modifies the post-yield response

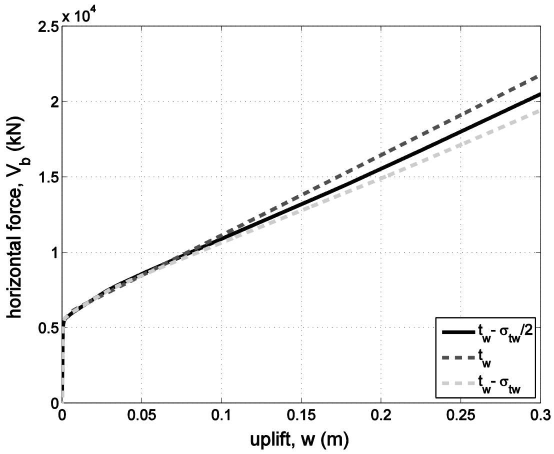

(g) t_w is important for large uplifts

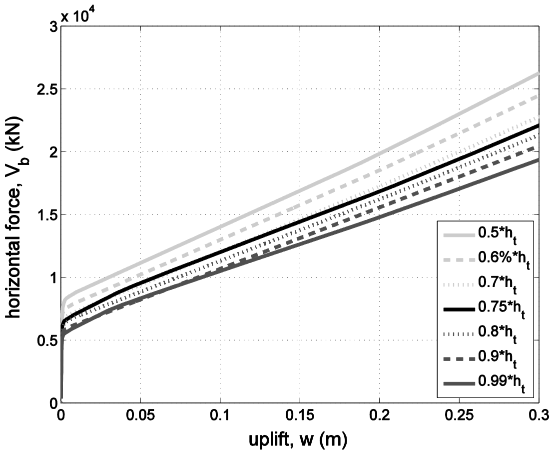

(h) increasing h_f reduces strength

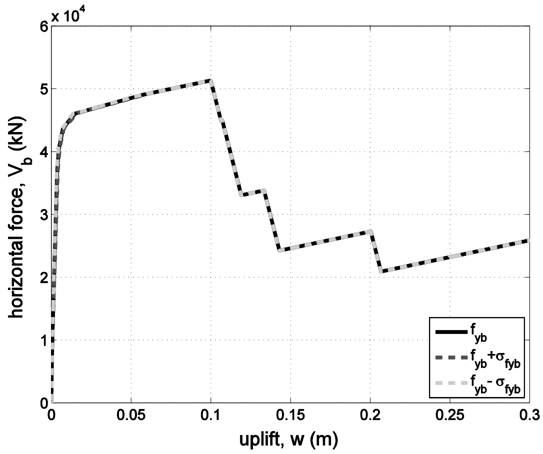

(i) f_{yb} is of minor importance

Fig. 13. Sensitivity analysis: Nonlinear Static Analysis.

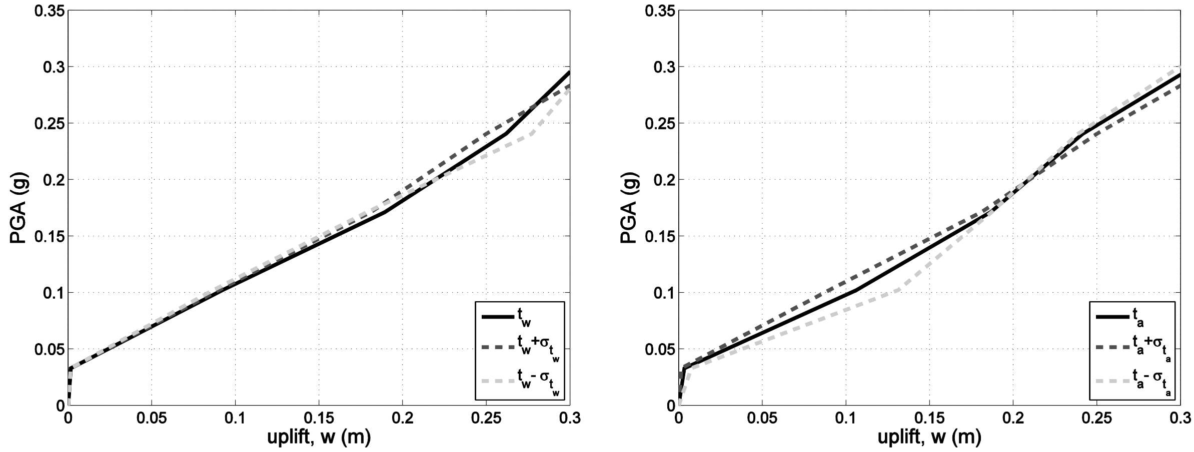

(a) t_w is of minor importance (b) t_a is of minor importance

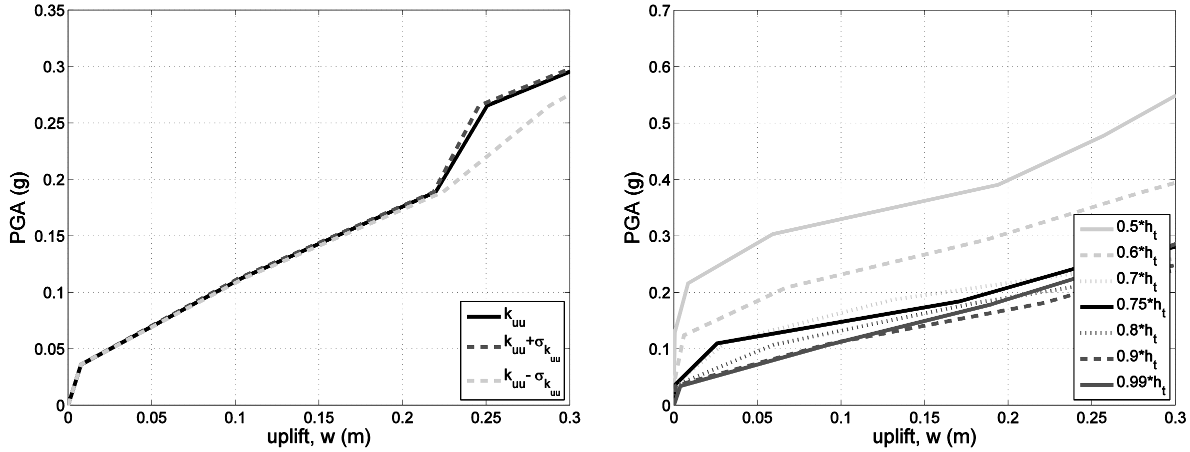

(c) k_{uu} is of minor importance (d) unexpected response for $h_f > 0.75h_t$

Fig. 14. Sensitivity analysis: Incremental Dynamic Analysis.

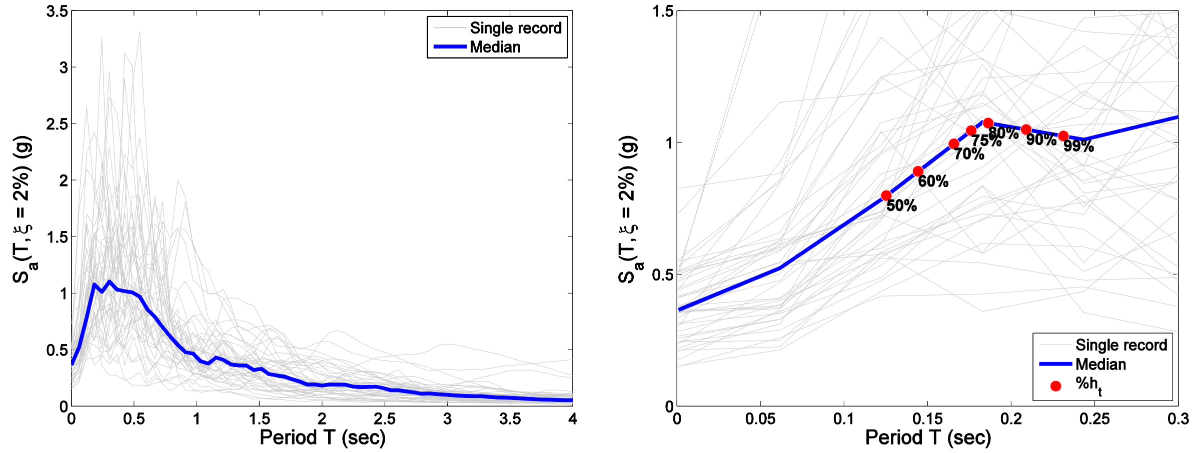

(a) (b)

Fig. 15. (a) Unscaled single record and median spectra (FEMA 2009) and (b) magnified view including the $0.5h_t$-$0.9h_t$ median $S_a(T_i)$ response.